CHALMERS

Fiber Engineering of Regenerated Cellulose Fibers

Master Thesis in the Master Degree Program, Biotechnology

FEIFEI DING

Department of Chemical and Biological Engineering
Division of Applied Surface Chemistry
Chalmers University of Technology
Gothenburg, Sweden 2011
Master Thesis 2011:10

Abstract

Cellulose, as the most abundant polymeric raw material, has been attracted to the industry for the past decades. To fully use the natural cellulose resource in a sustainable way a lot of work still needs to be done, thus the development of regenerated cellulose fibers is at a golden age. Looking briefly in the cellulose fiber history, many efforts have already been done, e.g. the viscose process from the early 20th century, the Lyocell process from the 80s, however their common drawback is the effect to the environment and the recycling abilities of the processes. In recent years, ionic liquids (ILs) as a kind of cellulose solvent in combination with other solvents or additives have been widely discussed all over the world both industrially and academically. Many novel fibers were produced from ILs. This project sees the cellulose from a different perspective which aimed to spin textile fibers from dissolved cellulose from 1-ethyl-3-methyl-imidazolium acetate (one of the well known ILs) and to manipulate the surface activities. To achieve this a series of dissolving and precipitation agents were tested. The fibers spun in the project were produced from different precipitation agents as well as additives, and characterized by a series of material characterization techniques. The results revealed that the structure can be manipulated by using precipitants with different polarities as well as with additives which have amphiphilic properties.

Acknowledgements

First I would like to thank Södra Innovation for giving me this chance to work with this project.

I would like to express my deepest gratitude to all the people involved in this project, here, I wish to thank:

Åsa Östlund, you are a very good friend to me rather than a teacher. You always encourage and comforts me whenever it is needed, a call or simply an SMS always comes at the right time. Carina Olsson, your great working attitude always inspires me.

Magnus Nydén, my examiner, though we haven't talked much, the short talks always inspired and encouraged me. Thanks for the great research environment you've created.

Many thanks to Caroline Löfgren for facilitating this diploma work and the time I've spent in Södra. Also thank Linda Friman who helped me a lot when I was in the lab at Södra.

Thanks Krister Holmberg for his time when I have had questions; Hanna Gustavsson for sharing her desk and office with me; Romain Bordes for helping me with the tensiometer instruments; Johan Karlsson and Christoffer Abrahamsson for helping me get the permission to run SEM; Matias Nordin for sharing the office at the start of the project; Ali Reza Movahedi for all the help in the lab; Lars Nordstierna for sharing the fume hoods with me; Ann Jakobsson for arranging all the practical stuff at TYK; Fredrik Gunnarsson for helping me with the freeze drier and of course many other people who work and study in the department. All together they have created a great working environment.

Great gratitude to Anders Kvist who helped me with the SEM/ESEM studies; Anne Wendel who helped with the ESCA experiments; Swerea for providing me the opportunity to learn to use the tensiometer for contact angle measurements; Christian Porsch at KTH for the help when I was in Stockholm introducing me to measure the contact angle on fibers, and Eugenio Ferrario from Artimplant for helping me with the spinning trials.

And also many thanks to my classmates from the biotechnology program for the great time we have been studied together. I wish you all a great future.

Finally I would like to thank my fiancée Joacim Kosonen and my family for always encouraging and supporting me

Feifei Ding
Gothenburg, February 2, 2012

Contents

List of Figures

List of Tables

List of Abbreviations

gg	gauche–gauche
gt	gauche–trans
tg	trans–gauche
BE	Electron binding energy
BMIMCl	1-*N*-butyl-3-methylimidazolium chloride
CA	Contact angle
DP	Degree of polymerization
EMIMAc	1-ethyl-3-methylimidazolium acetate
ESCA	Electron spectroscopy for chemical analysis
ESEM	Environmental scanning electron microscope
FEG	Field emission gun
GSED	Gaseous secondary electron detector
IL	Ionic liquid
KTH	Royal Institute of Technology
MCC	Microcrystalline cellulose
Mw	Molecular weight
NMMO	*N*-methylmorpholine-*N*-oxide
PEG	Poly(ethylene glycol)
RT	Room temperature

SDS	Sodium dodecyl sulfate
SEM	Scanning electron microscope
STS	sodium tetradecyl sulfate (STS)
TYK	Department of Applied Surface Chemistry
UTS	Ultimate tensile strength
XPS	X-ray photoelectron spectroscopy

1

Introduction

Due to the reduction of arable land and the depletion of oil resources, natural and synthetic fiber productions will face more and more constraints. At present, cellulose fibers have been taken into great account for both economical and environmental concerns for their abundant source in nature and the renewable and degradable properties.

1.1 Motivation

The most conventional and popular process of producing cellulose fibers is the viscose method which is over 100 years old and still dominates the cellulose textile fiber production (Klemm et al., 2005). The pulp with CS_2 is converted into cellulose xanthogenate as a metastable intermediate and later dissolved in sodium hydroxide in order to form a viscose solution in a wet process. However, the vast usage of auxiliaries (e.g. CS_2, NaOH, H_2SO_4) and fresh water as well as the emission of H_2S, CS_2 gases and heavy metals has caused intense pressure on the environment.

One of the alternative methods for fiber production is the NMMO (*N*-methylmorpholine-*N*-oxide) process which dissolves cellulose directly at concentrations of 10–15 wt % (Hermanutz et al., 2008). This was taken to commercial maturity with approximately 140,000 tons per year (Wendler et al., 2011), known as the Lyocell process. The Lyocell have stunning properties compared to viscose fibers, e.g. the strength in both dry and wet state, modulus of elasticity etc. Nevertheless, the main drawback of this process is the severe defibrillation behavior of the fibers which requires additional cross-linking processing (Hermanutz et al., 2008). Thus, this process has not yet replaced the viscose process to date.

Ionic liquid (IL), especially imidazolium salts, e.g. EMIMAc (1-ethyl-3-methyl-imidazolium acetate), which has a potential to be a new type of environmental friendly cellulose direct solvent is under investigation by many research groups all over the world.

Plenty of novel fibers spun from cellulose dissolved in ILs are reported (Li et al., 2010; Zhang et al., 2010; Tao et al., 2009; Cai et al., 2010; Feng and Chen, 2008) in recent years. Yet the physical properties of these fibers need to be improved.

1.2 Project description

The goal of this project was to spin fibers from dissolved cellulose in ILs and to manipulate the surface activities while spinning cellulose fibers in order to control the hydrophobicity. To achieve this, a series of dissolving and precipitation agents were tested. The material properties (for example, surface structure and morphology, hydrophilicity/hydrophobicity and fiber strength) were measured by a series of techniques e.g. SEM/ESEM, ESCA, tensile testing and contact angle measurements.

The aim was to produce a new type of environmental cotton like textile fibers.

The hypothesis was that the hydrophobicity of the fiber surface may be directed by different precipitation agents at different polarity (polarity index: water > ethanol > acetone > propanol > peptane) as well as by adding some known surfactants into the spin dope due to the amphiphilic property of the cellulose molecules.

1.3 Background

Cellulose, as the most abundant polymeric raw material, has been attractive to the global industry in many aspects over the past decades worldwide e.g. paper making, pharmaceuticals, foodstuffs, textiles etc. It has versatile properties such as hydrophilicity, chirality, biodegradability, biocompatibility etc. (Klemm et al., 2005). General information about cellulose and characterization techniques will be presented in this chapter.

1.3.1 Cellulose

The structure of cellulose can be described as a carbohydrate polymer with repeating D-glucose units which are covalently linked through $\beta(1 \rightarrow 4)$-glycosidic bonds (Fig.1.2a). Thus, cellulose is a polymer with multiple hydroxyl groups which form hydrogen bonds with oxygen atoms on the same or an adjacent chain, holding the chains firmly alongside each other. In other words, the cellulose molecules form long, straight chains which are strengthened by intramolecular hydrogen bonds and van der Waals interaction, which pack together to form crystalline structures. French et al. (1993), Cousins and Brown Jr. (1995) also showed that the hydrophobic groups contributed to the crystal stability by calculating the inter- and intramolecular energy for cellulose forms.

Due to its supra-molecular structure, the solid state of cellulose reveals as both crystalline (high order) and amorphous (low order). The crystalline structure of native cellulose appears as cellulose I, presenting in two polymorphs: triclinic ($I\alpha$) and monoclinic ($I\beta$) which appear alongside each other. The $I\alpha/I\beta$ ratio varies in different origins of cellulose, e.g. cellulose produced by primitive organisms consists mostly $I\alpha$ while higher plants have the $I\beta$ dominant (O'Sullivan, 1997). Corresponding to the inter- and intra-

molecular hydrogen bonds, cellulose may occur in other crystal structures, e.g. cellulose II, III and IV. By treatment with aqueous sodium hydroxide (mercerization) or by dissolution of the cellulose followed by precipitation, cellulose II which has an antiparallel orientation, in contrast to native cellulose parallel chains, (Figure 1.1) can be formed. The conversion cannot be reversed, indicating that cellulose II is more stable. Cellulose III and IV can be produced by treatment with various chemicals and in combination of heating and pressure (O'Sullivan, 1997; Klemm et al., 2005).

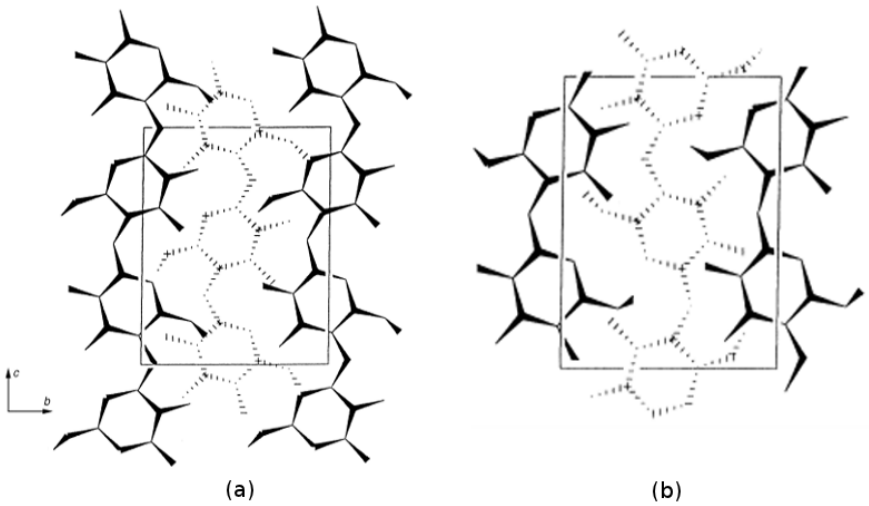

Figure 1.1: Projection of a two-chain model of cellulose I and II. (a) cellulose I: parallel orientation; (b) cellulose II: anti–parallel orientation. (Figures are adapted from O'Sullivan (1997))

The properties and numerous applications of cellulose depends highly on its chain length and its fiber morphology. The chain length, i.e the number of glucose units, varies with the origins and the chemical treatment of the raw materials. The chain length for a cellulose from wood pulp is between 300 and 1700 units; cotton and other plant fibers have the values ranging from 800 to 10,000 units; bacterial cellulose are observed to have similar range as cotton and other plant fibers. The number of the repeating units of the regenerated cellulose varies depending on the dissolution/regeneration process, Klemm et al. (2005) reviewed that it is about 250–500. Powdery cellulose can be produced from partial chain degradation, yielding chain length of 150–300 units, e.g microcrystalline cellulose.

As a perspective on the directional chemical asymmetry, the cellulose chain consists one nonreducing end which is a D–glucose unit with a C4–OH group (Figure 1.2a left side); in order to be in equilibrium with the aldehyde structure, the other end is terminated with a free hydroxyl group at C1 (the reducing end) (Figure 1.2a right side) (Klemm et al., 2005). This asymmetry plays a significant role in the processing of cellulose in terms of isolation and purification processes.

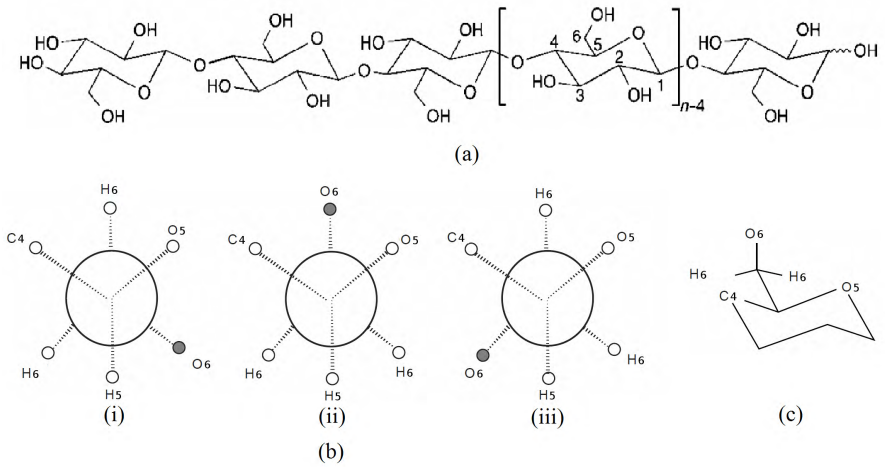

Figure 1.2: Molecular structure and conformation of cellulose. (a)molecular structure of cellulose. (n refers to degree of polymerization); (b)the three possible minimum energy orientations of the hydroxymethyl group: (i) gt, (ii) gg, (iii) tg; (c) part of a single repeating glucose unit (without the hydroxyl groups). (Adapted from Klemm et al. (2005); O'Sullivan (1997))

The inter- and intra- molecular hydrogen bonds play an import role in determining the structure of the cellulose. Considering hydrogen bonds, close attention should be drawn to the rotational conformation of the hydroxyl group at C6. There are three possible conformations that O6 can adopt, shown in Figure 1.2b. These staggered domains are referred to in the literature as gauche-trans (*gt*) where O6 is gauche (60°) to O5 and trans (180°) to C4, gauche–gauche (*gg*) where O6 is gauche (60°) to O5 and C4, and trans–gauche (*gt*) where O6 is trans (180°) to O5 and gauche (60°) to C4 respectively. As is described in the literature, cellulose I has a *tg* conformation while cellulose II has the *gt* conformation is more likely to occur than the *gg*. Suggested intra- and intermolecular hydrogen bondings are shown in Figure 1.3 (O'Sullivan, 1997).

Cellulose is insoluble in water and in most conventional organic solvents. Most of the literatures agree on that the insolubility of cellulose is due to the hydrogen bonding between cellulose and the solvent. However Lindman et al. (2010) has another explanation on that, which is that the amphiphilic property of the cellulose draws strong attention to the hydrophobic interactions which may result in low aqueous solubility. Yamane et al. (2006) also reported the hydrophobic nature of cellulose from a structural point of view.

1.3.2 Cellulose solvents and ionic liquids

In the past few decades, the utilization and development of natural resources have been attractive fields for scientists to focus on. Cellulose, as the most abundant and versatile raw material, has been widely used to make textiles, paper and food fillers. However as

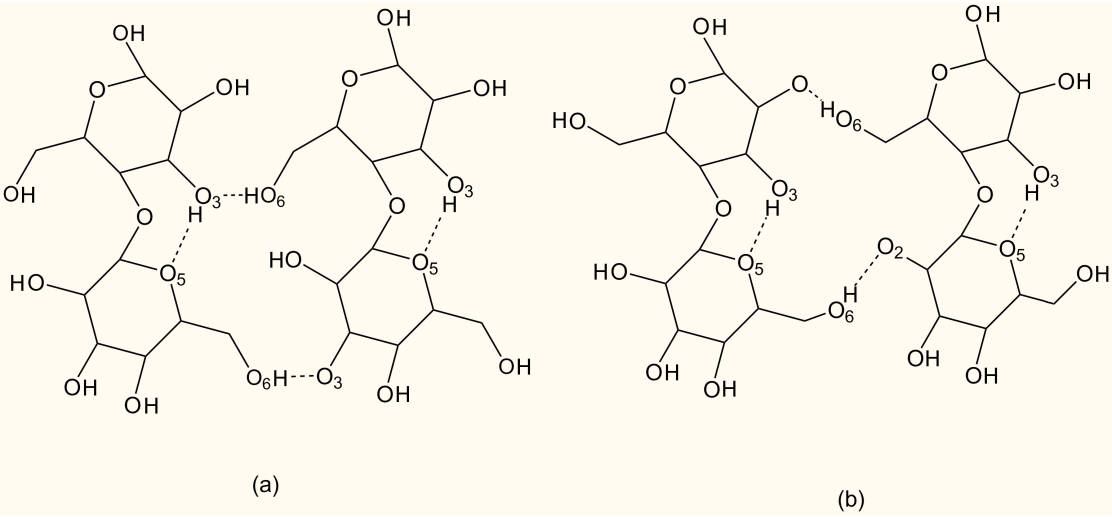

Figure 1.3: Suggested hydrogen bonding for cellulose I (a) and II (b). (Adapted from O'Sullivan (1997))

described previously, cellulose is very difficult to dissolve in water and most conventional organic solvents, which causes a lot of difficulties for its utilization and developments. From an environmental and sustainable point of view, the regeneration of cellulose which requires dissolving process also calls for development of cellulose solvents.

Generally, to dissolve cellulose, the cellulose inter- and intra- molecular interactions need to be weakened and there are two ways to achieve this. One alternative is to make cellulose derivatives, e.g. the method used in the viscose process which yields cellulose xanthate as its product. However this kind of process usually emits a great deal of pollution, and thus is not environmental friendly. The other alternative is to dissolve cellulose directly in some special solvents, e.g. NMMO which is used in the Lyocell process.

ILs refers to salts with low melting points usually less than 100 °C and contain large volume cations and anions. The ILs have been used in several fields e.g. extraction process, solar cell, food and bio–products etc. (Kosan et al., 2007). The versatile and exceptional properties (varies for different ILs) such as chemical and thermal stability, non–flammability, non–volatile properties, and great dissolving capability, make ILs to potentially be a "green solvent" for cellulose (Cai et al., 2010). Imidazolium based salts are the ILs most are discussed in the literature. EMIMAc (Figure 1.4) is one of the most popular ILs for dissolving cellulose. Novel fibers with similar properties to the Lyocell fibers can

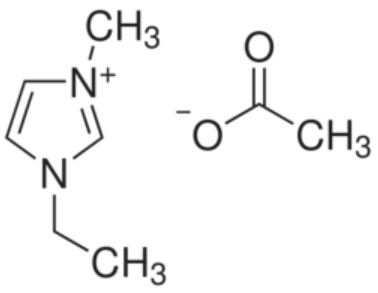

Figure 1.4: Chemical structure of EMIMAc

be produced from cellulose/EMIMAc solution. Compared with some other widely used ILs such as BMIMCl (1-*N*-butyl-3-methylimidazolium chloride), EMIMAc is liquid under ambient temperature, gives low viscosity and higher miscibility with cellulose at lower temperature and takes up to 20 wt% cellulose (Lovell et al., 2010). Thus EMIMAc provides a promising solvent for cellulose processing.

1.3.3 Characterization techniques

Surface morphology

Figure 1.5: The FEI Quanta™ ESEM equipment at MC2, Chalmers

One of the most common techniques for surface morphology studies is scanning electron microscope (SEM), which can give information about the chemical composition, morphology and different structures in the sample. Instead of a light–beam which is used as an ordinary light–microscope, SEM produces an electron-beam which is focused by going through both lenses and magnetic fields before it strikes the sample. Some electrons, but also X-rays, are ejected from the sample. These X-rays and electrons are collected by a detector which produces an 2D image (Schweitzer, 2010; Swapp, 2010). It allows for magnification at higher levels, since it has much higher resolution, and it is easier to have a wider focus for that this type of microscope has a large depth of field (Schweitzer, 2006).

SEM works under vacuum conditions to prevent e.g. dust to interfere. An electron gun generates an electron beam which is focused by condenser lenses and passed through deflection coils. When the sample is hit by the high intensity electron beam, information is available from the secondary electrons, X-rays, light and back–scattered electrons(Swapp, 2010). Depending on which detector is used, different data is collected and used for gaining information about the sample. Such information is usually surface topography, morphology, chemical composition, conductivity etc. The resolution can be as good as down to 1 nm. One important factor to consider is the voltage of the beam. Higher voltage increases the resolution but decreases the surface sensitivity since the beam penetrates deeper into the sample.

An ESEM (environmental scanning electron microscope) is similar to a SEM but allows the specimens to be "wet", uncoated, in other words, it is unnecessary to make nonconductive samples conductive, which is considered as an advantage to the SEM. It also enables dynamic experiments with the ESEM in wet mode. The high vacuum which is critical in SEM is not required in ESEM and the Peltier heating/cooling stage provides an environment with 20 °C above or below ambient temper-

Figure 1.6: The Leo Ultra 55 FEG SEM equipment at MC2, Chalmers

ature and 100% relative humidity at the sample surface.

Water vapor is used as an imaging gas in the specimen chamber. First the water vapor is introduced to the specimen chamber by a vacuum pump which controls the chamber pressure. The primary energetic electron beam penetrates the cloud water vapor with little apparent scatter, scanning through the specimen surface, the secondary electrons are then released from the surface. When the water vapor molecules are struck by the secondary electrons, they produce secondary electrons themselves and then in turn strike other water vapor molecules producing secondary electrons. As a result, a cascade of secondary electrons are produced by the water vapor, in other words, the original secondary electron signal were amplified by the water vapor. The amplified signal is then attached to a GSED (gaseous secondary electron detector) with its positive charge then forces the positively charged water ions towards the negatively charged specimen surface thus neutralize the specimen surface (Wallace and Robinson, 2011).

However in order to get an perfect image, some adjustments need to be done including the voltage, spot size, vapor pressure, working distance etc. and such adjustments need time and experience.

For cellulose, the beam from SEM may easily destroy the specimen surface, so the ESEM is also considered for the surface morphology characterization in the study.

Fiber strength

In a tensile test, the determination of how a material reacts to forces can be done in a short range of time. By pulling the material, its strength will be found along how much it will elongate. A complete tensile profile will be received by pulling the material until it breaks. A point of much interest is when failure occurs and is called "Ultimate Tensile Strength (UTS)" (DeGarmo et al., 2002). The result is independent on the size of the specimen but depends on the preparation of the specimen and the surrounding temperature (Smith and Hashemi, 2005).

Two concepts usually associated with tensile testings are Hooke's law and modulus of elasticity. In most cases of tensile testing, the relationship between applied load and the elongation will be linear in the initial part of the test, and this relationship is defined as Hooke's law, where the ratio of stress (σ) to strain (ε) is constant. Modulus of elasticity (E) is only valid for the linear region of the curve and is a measure of the stiffness of the material. If the load is removed within this region, the material will recover to its original condition; otherwise some permanent deformation will remain (DeGarmo et al., 2002).

Contact angle

Contact angle (CA) (θ) reflects the wettability of a material. Considering a liquid drop on a solid surface, the CA is defined geometrically as the angle formed by the droplet at the interfaces between gas and solid. Figure 1.7 illustrates the CA on different surfaces. Take a water droplet for example, at low CA the liquid is strongly attracted to the

surface indicating that the surface is hydrophilic, a less hydrophilic solid will give the CA up to 90° a surface is considered to be hydrophobic if the CA is larger than 90°.

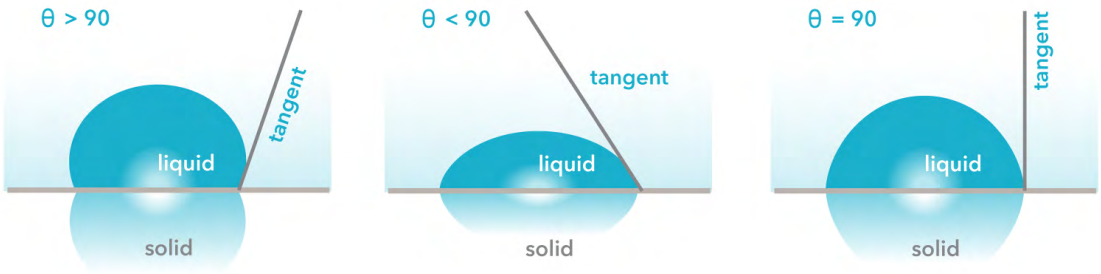

Figure 1.7: The CA on different surfaces.

A flat surface is usually measured by an optical tensiometer by which the shape of the droplet is captured by a camera and the CA can be directly assessed by measuring the angle formed between the solid and the tangent to the drop surface (see Figure 1.7). This method is usually used for measuring CA on flat surfaces like films, membranes and paper.

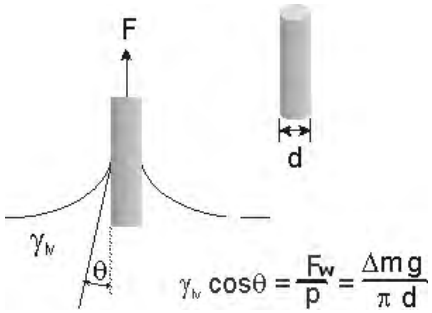

Figure 1.8: Scheme of wetting and wetting force. (Grundke et al., 2011)

The dynamic Wilhelmy plate method has been extensively applied to solid–liquid CA measurements and is also used for measuring CA on fibers. It measures the CA when the three–phase boundary (liquid/solid/vapor) is in motion. A small piece of microfibril is prepared and held vertically on the balance, tarred, moved towards the beaker containing the wetting agent. Once the fiber is in contact with the liquid the change in force will be detected and recorded by the device which value is set to be zero depth of immersion. As the fiber is immersed deeper into the liquid the forces on the balance ($F_{total} = wettingforce + weightoffiber - buoyancy$) are recorded. The sum of the wetting force can be given by Equation 1.1 (Erbil, 2006).

$$F_{total} = p\gamma_{LV}cos\theta + mg - \rho g\frac{1}{2}pd \tag{1.1}$$

where F_{total} is measured by the device, m is the mass of the fiber, g is the acceleration of gravity, ρ_L is the liquid density, p is is the perimeter, γ_{LV} is the liquid surface tension and θ is the CA at the interface between the liquid and the solid. Since the weight of the fiber is tarred and the the force extrapolated by zero depth immersion the effect of weight and buoyancy force can be removed. The remaining wetting force (F_w) is given by Equation 1.2. When the liquid is extremely hydrophobic the $cos\theta$ tends to be 1 and

the perimeter can be also obtained from Equation 1.2 (Gupta, 2000).

$$F_w = \gamma_{LV} p cos\theta \tag{1.2}$$

Thus the force data can be received and used to calculate the CA. The CA that is recorded as the fiber advances into the liquid is the advancing CA while the receding CA is the CA recorded as the fiber retreats from the liquid. The process is illustrated graphically as in Figure 1.9 (Erbil, 2006; Attension, 2011).

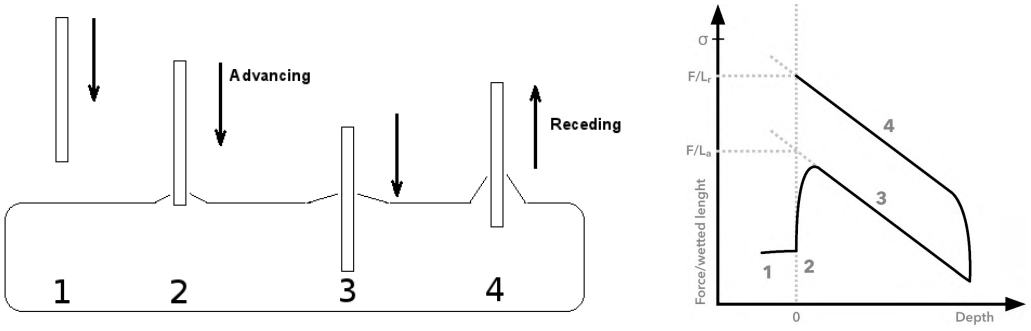

(a) The progress of the Wihelmy plate measurements

(b) Graph of force/wetted length vs depth of immersion

Figure 1.9: The CA measurements using the Wilhelmy plate method. 1- The sample is above the liquid; 2- the sample is in contact with the liquid surface; 3- the sample is immersed, the force changes which is caused by the buoyant force is recorded; 4- after having reached the desired depth the sample is retreating from the surface and the receding angles are recorded.

However the measurements require to use high purity of the liquid, every time the fiber is in contact with the liquid the surface tension of the liquid is changed due to contamination. The sample must be cut in a regular geometry and hung exact vertically when contacting the surface. It should also be extremely clean to be able to get accurate data, small contamination on the surface affects the result a lot.

Surface chemical analysis

Electron spectroscopy for chemical analysis (ESCA), also known as XPS (X-ray photoelectron spectroscopy) is a surface chemistry analysis technique which characterizes the surface chemistry of a material under a certain condition, for example, fracturing, heating etc. The ESCA equipment provids an ultrahigh vacuum environment and a low–energy monochromatic X-ray source which the sample is exposed to. The X-ray beam causes the ejection of core–level electrons from sample atom. By measuring the kinetic energy and number of electrons that escape from the top 1 to 10 nm of the sample, an photoelectron spectrum is obtained.

The BE (electron binding energy) can be calculated by Equation 1.3 (Bancroft, 2011).

$$E_{binding} = E_{photon} - (E_{kinetic} + \phi) \tag{1.3}$$

where $E_{binding}$ is the BE of the electron, E_{photon} is the energy of the X-ray photons, $E_{kinetic}$ is the kinetic energy of the electron which is measured by the instrument and ϕ is the work function of the spectrometer (Bancroft, 2011).

The BE value of an electron depends not only on the photoemission but also the oxidation state of the atom and the local chemical and physical environment (Fairbrother, 2004). Withdrawal of valence electron charge give rise to the BE value while addition of valence electron charge reduces the BE value, such changes in the BE values are so called chemical shifts which can be visualized, thus the chemical structure is interpreted.

2

Experimental Part

The experimental part, material preparation, spinning trials and characterizations for fibers and films are described in this chapter.

2.1 Materials

Avicel PH 102 microcrystalline cellulose (MCC) with the DP (degree of polymerization) of no more than 350 glucose units (provided by manufactures) were used in this work as the cellulose source. EMIMAc (97%) produced by BASF was purchased from Sigma–Aldrich and was used as the IL in this work.

Additives with amphiphilic properties are believed to have the potential to manipulate the surface of fibers/films while the cellulose is aggregated during coagulation. When choosing the additives, poly(ethylene glycol) (PEG) and sodium dodecyl sulfate (SDS) were taken into consideration.

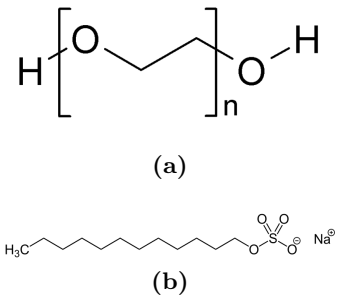

(a) **(b)**

Figure 2.1: Molecular structure of PEG and SDS

PEG (Figure 2.1a) is widely used in the industry from manufacturing to medicine. The role of PEG molecules is believed to be the acceptor of hydrogen bonds which connects the hydroxyl groups in cellulose and prevents the aggregation of cellulose (Zhang et al., 2010). As a result the viscosity is reduced. SDS, as an anionic surfactant, has been widely used in cleaning and hygiene products. As shown in Figure 2.1b, SDS consists of a 12-carbon tail which is attached to a sulfate group, resulting in the amphiphilic property. PEG with Mw (Molecular weight) 300 and SDS were purchased from Sigma–Aldrich.

2.1.1 Precipitation agents

The precipitation agents were selected according to their polarities which were used in the experiments were normal tap water, 99.5% ethanol, 99% 1-propanol, 99.5% acetone and 99% heptane.

2.2 Preparation of the solutions

The MCC, EMIMAc as well as the additives were weight according the concentration listed in Table 2.1. The cellulose/EMIMAc solution was prepared by gradually adding MCC powders into the preheated EMIMAc at the temperature around 60 °C during stirring until the MCC was fully dissolved and formed a homogeneous solution. Then the additives were also added as is described previously for the cellulose.

In order to get a less viscous solution, the solutions were preheated at about 60 °C in a water bath every time before use.

2.3 Experimental setup

2.3.1 Trials in the lab

In order to successfully spin fibers through a wet-spinning process, a serials of precipitation trials were carried out in the lab. Firstly the miscibilities of precipitation agents and EMIMAc were tested by putting EMIMAc droplets into the precipitation agents (i.e. water, ethanal, propanol, acetone and heptane) in this work. Then a serials of films and "home made" fibers were made by precipitating the cellulose/EMIMAc solution in the precipitation agents (Figure 2.2). The samples were air–dried at room temperature for at least two days until further characterizations were performed. A detailed manual for making the films can be found in Appendix A.1.

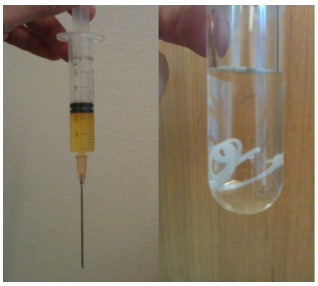

Figure 2.2: "Home made" fibers

There were two groups of trials: (a) trials with different coagulants (Figure 2.3a) and (b) trials with additives (Figure 2.3b). For the former one, the cellulose/EMIMAc

Table 2.1: Solution concentrations

Cellulose (%)	EMIMAc (%)	SDS (%)	PEG (%)
4	96	—	—
4	92	4	—
4	92	—	4

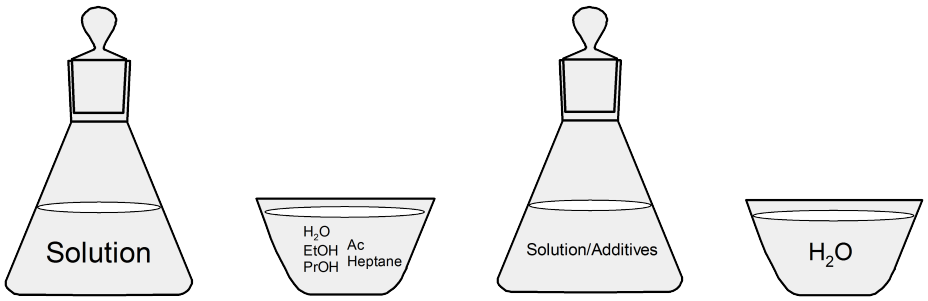

(a) Trials with different coagulants **(b)** Trials with additives

Figure 2.3: Experimental setup. (a) The cellulose/EMIMAc solution (on the left) was precipitated in water, ethanol, propanol, actone and heptane repectively; (b) the cellulose/EMIMAc solution was mixed with additives and precipitated in water only.

solution was precipitated in water, ethanol, propanol, actone and heptane respectively while for the latter one, the cellulose/EMIMAc solution with additives (SDS and PEG in this work) was precipitated in water.

2.3.2 Spinning trials

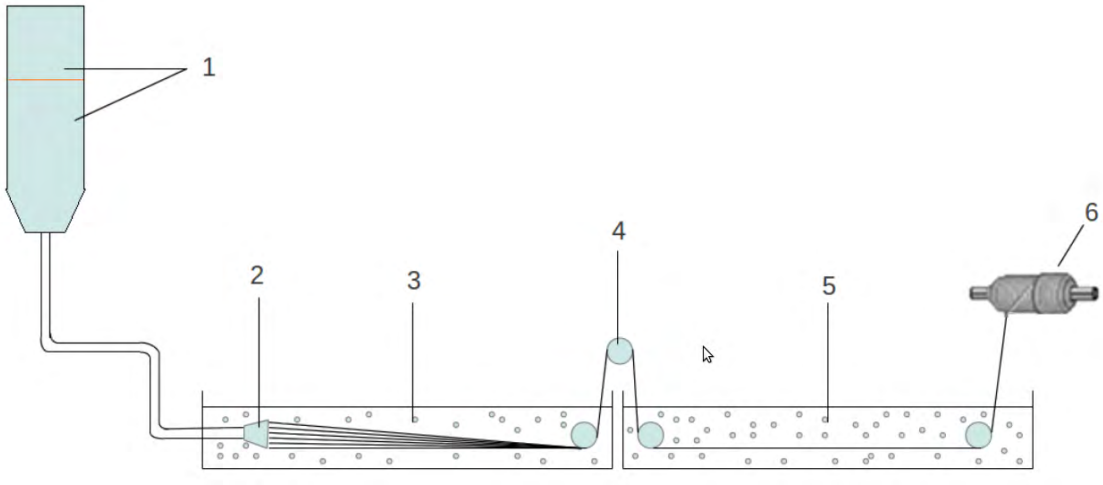

Figure 2.4: Sketch of a wet–spinning setup. 1- Spinning dope in a stainless cylinder attached to a pressure extruder; 2- spinneret (120 holes $\times\phi 80\mu m$); 3- coagulation bath (T1); 4- godet (v); 5- washing bath (hot water, T2); 6- collector.

The spinning trials were performed through a wet–spinning machine at Artimplant AB, Västra Frölunda, Sweden. A sketch of a wet–spinning set up is illustrated in Figure 2.4. The selected coagulants and additives were used in the spinning trials according to the trials performed in Section 2.3.1.

Table 2.2: Parameters for the spinning trials. C: cellulose; E: EMIMAc; T1: temperature of the first bath (No.3 in Figure 2.4); T2: temperature of the second bath (No.5 in Figure 2.4); v: the stretching speed after the first bath (No.4 in Figure 2.4).

	H2O			EtOH			PrOH		
	T1 (°C)	T2 (°C)	v (m/min)	T1 (°C)	T2 (°C)	v (m/min)	T1 (°C)	T2 (°C)	v (m/min)
C/E	RT	72.5	Manual (∼1.0)	RT	55	1.0	RT	72.6	1.0
C/E	67	80	1.36						
C/E+SDS	62	∼70	1.6	—	—	—	—	—	—
C/E+PEG	75	∼70	1.52	—	—	—	—	—	—

In each spinning trial, the solution together with the sample holder and the spin dope (No.1 in Figure 2.4) was extruded from the spinneret (No.2 in Figure 2.4) into the coagulation bath (No.3 in Figure 2.4) containing the selected coagulant. The fiber was guided by a tweezers to the godet (No.4 in Figure 2.4) which provided the tension for elongation and stretching at a certain velocity (v) to enhance the fiber strength. Then fiber was washed in hot water at about ∼70 °C (No.5 in Figure 2.4) and finally wrapped to a roller (No.6 in Figure 2.4). In an up–scale fiber processing the elongation, the stretching procedure is repeated while in the washing bath which velocity varies depending on the production.

It should be noticed that the solutions were precipitated in different coagulation baths at room temperature (RT) while the those with additives were performed at around 65 °C. Detailed parameters for the spinning process are listed in Table 2.2.

The fibers were collected and air–dried until further characterizations. To make sure no ILs remains in the spun fibers, the fibers were washed by soaking the fibers in their relevant coagulants, e.g. water, ethanol, propanol etc. for one week and air–dried again for further characterizations.

2.4 Characterizations

The fiber properties, i.e. surface structure and morphology, fiber strength, hydrophilicity/hydrophobicity and surface chemical compounds were analyzed by a series of material characterization techniques.

2.4.1 Surface morphology

The SEM session for the surface structure and morphology properties was carried out by a Leo Ultra 55 FEG (Field emission gun) SEM (Figure 1.6) and ESEM was performed by FEI Quanta^{TM}200 FEG ESEM (Figure 1.5). Both the SEM and ESEM equipment are available at the Department of Microtechnology and Nanoscience, Chalmers.

Before running the SEM/ESEM, the fibers were cut into small fragments and carefully separated to get single microfibrils, while the films were cut into approximately 1 cm in diameter or width. For SEM, the prepared the samples were glued to a microscopy plate with a carbon tape, following by sputtering with a thin gold layer with a vacuum sputter–coater to improve the conductivity of the samples and also to protect them against the electron beams. A voltage at 3–5 keV was used to image the fibers and films. The correct focus and magnification was found to obtain as good pictures as possible. For ESEM, the analysis was done under low vacuum (0.6 torr), voltage 10.0 kv and spot size was 3.0.

2.4.2 Fiber strength

The fiber strength were tested by a tensile testing machine produced by Zwick Roell at Södra Innovation, Värö. A serials of values were obtained from the software: load at break (N), elongation at break (%), stiffness (N/mm).

One meter of each fiber, i.e. a bundle of fibrills, was weighted in a laboratory scale in order to get the fiber tex value (unit $g/1000m$), thus the real strength — tenacity (cN/tex). The tenacity is calculated by dividing the load at break by tex.

2.4.3 Contact angle measurements on films and fibers

The hydrophilicity/hydrophobicity was tested through contact angle measurements on films and fibers.

The CA on films were measured by a dynamic CA tester (DAT 1100 Fibro System AB, Sweden) which measures initial hydrophilicity/hydrophobicity and the dynamic change of CA and volume over time. An optical tensiometer (Theta, Attension, Biolin-Scientific) was also used to measure the CA, which measures static CA on a single film. Water and hexadecane were used as the wetting agents.

The Wilhelmy balance measurements of CA on fibers were carried out using a Cahn DCA–322 (Cahn Instruments, Inc.) equipped with the appropriate software at the Department of Fiber and Polymer Technology, KTH. Water and hexadecane were used as the wetting agents.

2.4.4 Electron spectroscopy for chemical analysis

To check if there were IL left in the fibers, ESCA at Chalmers Science Park was used to analyze the chemical character of the fiber surface. The analysis was done on the surface down to 5 nm and the BE values were recorded.

3

Results and Discussion

The results from the trials in the lab, characterizations of surface morphology studies, fiber tensile testings, ESCA analysis and the measurements of CA are listed in this chapter. Noticing that the scale of the ESEM images can be only reached up to 10 μm and the image revealed no significant difference from the SEM images from which the samples were coated with a thick layer of gold, only the images taken by SEM are shown.

3.1 Trials in the lab

It is believed that the coagulation of the spin dope for making fibers, or the solution for making films is a simple physical sol–gel transition process which involves two kinds of motions: one is the solvent (in this case the EMIMAc) leaving the cellulose solution while the other is the non–solvent (in this case the chosen precipitation agent) diffuses into the cellulose solution. The miscibility is usually affected by the polymer solution, coagulation bath composition, coagulation bath temperature and the stretching speed (Chen et al., 2007).

The miscibility trials showed that EMIMAc and the coagulants, H_2O and EtOH both mixed completely; PrOH and acetone mixed completely with EMIMAc as well but the effort of stirring or shaking was needed; heptane did not mix with EMIMAc at all after a few minutes of shaking. Therefore H_2O, EtOH, PrOH and ACT was chosen for further trials.

It was shown that all the chosen coagulants could form films. However when extruding the cellulose/EMIMAc solution into the acetone solvent, the difference in density made the solution to fall quickly down to the bottom of the glass tube and no fiber could be formed, while other solvents all formed fibers successfully as well as for the solutions with additives. Table 3.1 summarizes the results for the trials in the lab of home–made films and fibers.

Table 3.1: Summary of the trials in the lab. √ successful; × unsuccessful; — not done. C: cellulose; E: EMIMAc

Spin dope	Coagulants							
	H2O		EtOH		PrOH		ACT	
	Film	Fiber	Film	Fiber	Film	Fiber	Film	Fiber
C/E	√	√	√	√	√	√	√	×
C/E+SDS	√	√	—	—	—	—	—	—
C/E+PEG	√	√	—	—	—	—	—	—

3.2 Structure and Morphology

The SEM images reveal that all fibers span at Artimplant had a dense and homogeneous structure with a strip shape along the direction of the flow during spinning.

Among the fibers spun in different coagulants, H_2O as a coagulant seems to give a smoother surface of the fiber while there were no significant differences between the fibers spun in EtOH and PrOH (Figure 3.1) though PrOH seems to give a grainier surface when looking at a larger magnification (Figure 3.2). It is already shown in the lab trials that the lower polarity the solvent has, the less it dissolves EMIMAc. During the spinning process, the miscibility between water and EMIMAc was the highest when comparing to other solvents, thus the cellulose solidifies the quickest, resulting in a smoothest surface while propanol was the slowest, giving the surface more roughness.

Figure 3.3 and 3.4 are the images for the fibers spun in hot water with and without additives. It shows that SDS gives a smoother surface to the fiber while there was no significant difference between the fibers spun with and without PEG. Since cellulose is amphiphilic, it tends to hold the hydrophobic tail of the SDS inside its hydrophobic rings, leaving the hydrophilic head to interact with the water, i.e. the coagulant. The EMIMAc also interacts with the cellulose but diffuses out into the water, leaving the cellulose to self–assemble by the hydrophobic interactions, thus forming a smooth surface.

Compared with the two groups of fibers, i.e. spun with different precipitation agents and with additives in the spin dope, the fibers spun with additives exhibit a smoother surface. It should be noticed that the fibers spun with additives were carried out in hot water, whereas EtOh and PrOH were held at room temperature. Therefore, only the fibers spun in H_2O were comparable through the EtOH and PrOH baths at room temperature. However the fibers spun in hot water show slightly smoother surface compare to those spun in water at room temperature. Chen et al. (2007) reported that the coagulation rate of the solvent and nonsolvent increases while temperature increases. When the fibers were spun in hot water, the miscibility of EMIMAc and H_2O was increased, leading to faster cellulose aggregation, thus results in a smooth surface which shape was

determined by the spinning spinneret.

The films in Figure 3.5 and 3.6 were all made by precipitating the solution into the coagulants at room temperature. It is shown that the films got a homogeneous surface with a structure like dry cracked ground. PrOH seems to give much rougher surface compared to H_2O and EtOH, and EtOH gives a denser surface than H_2O. It should also be noticed that the films made from PrOH were not as transparent as other films. The films with PEG had a rougher surface while the films without additives had more dense cracks compare to those with additives. The images seem not very comparable to those from the spun fibers due to the coagulation conditions, for example the temperature, the volume of the coagulant, the coagulation time and the physical stretch which the fibers had while the film did not. Therefore more controlled spinning and film making processing procedures are needed.

To summarize the outcome of the film casting, it seems like that slow coagulation gives more strcture to the film, i.e. more cracks.

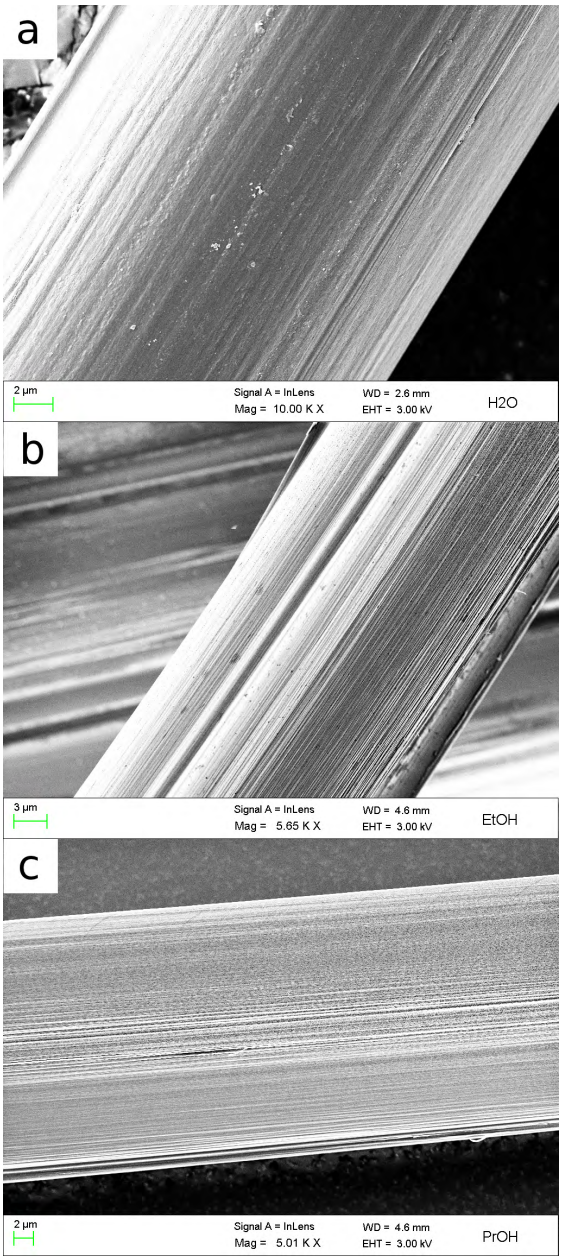

Figure 3.1: Fibers spun in different coagulants shown at smaller magnification. a. H_2O, scale bar = 2 μm; b. EtOH, scale bar = 3 μm; c. PrOH, scale bar = 2 μm

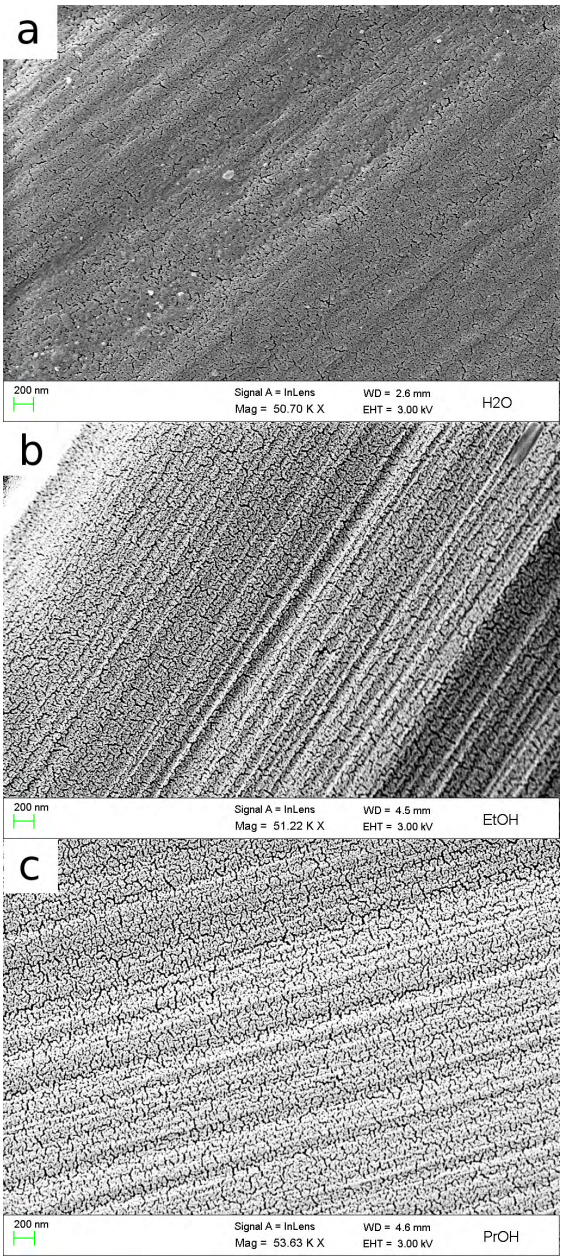

Figure 3.2: Fibers spun in different coagulants shown at lager magnification. a. H_2O, scale bar = 200 nm; b. EtOH, scale bar = 200 nm; c. PrOH, scale bar = 200 nm

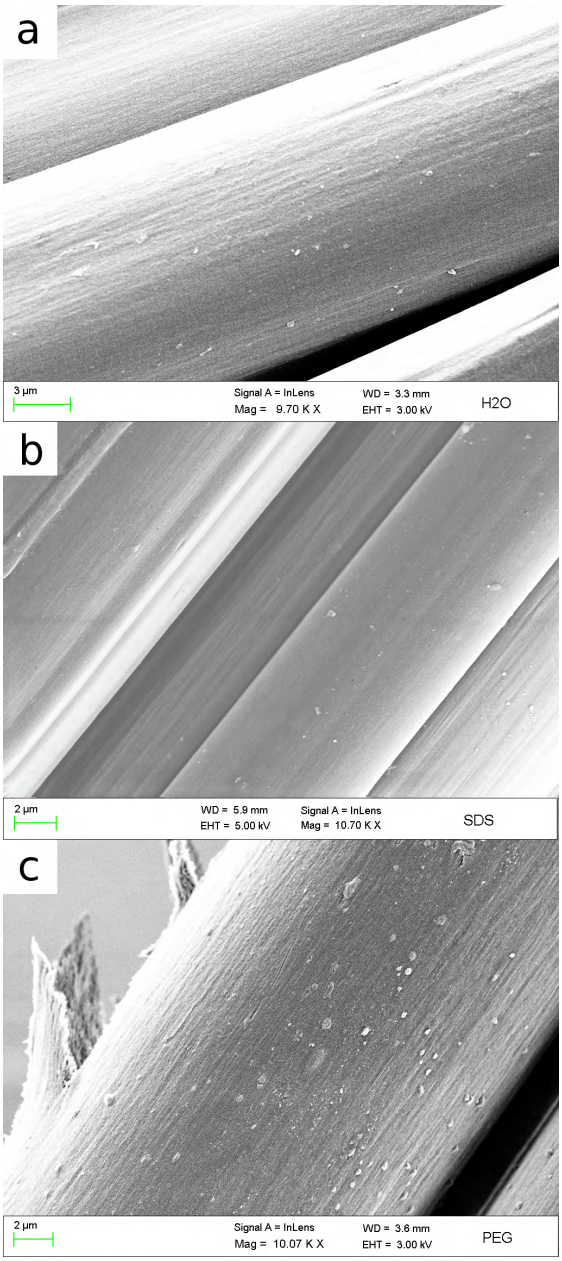

Figure 3.3: Fibers spun in hot H_2O with additives shown at smaller magnification. a. solution of cellulose/EMIMAc, scale bar = 3 μm; b. solution of cellulose/EMIMAc with SDS, scale bar = 2 μm; c. solution of cellulose/EMIMAc with PEG, scale bar = 2 μm

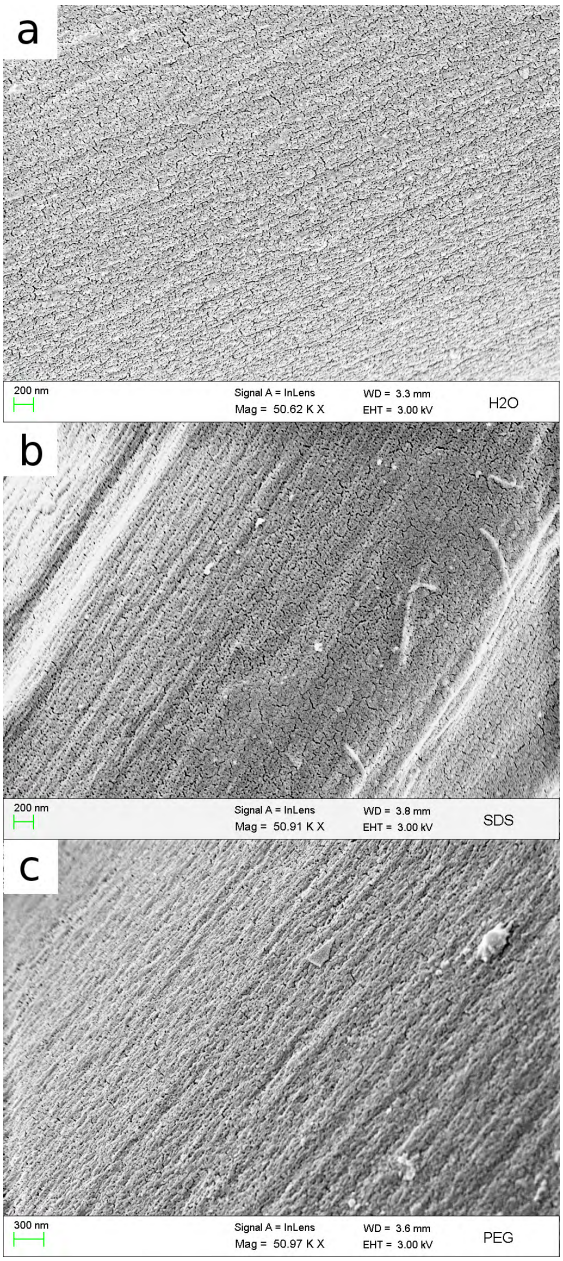

Figure 3.4: Fibers spun in hot H_2O shown at lager magnification. a. solution of cellulose/EMIMAc, scale bar = 200 nm; b. solution of cellulose/EMIMAc with SDS, scale bar = 200 nm; c. solution of cellulose/EMIMAc with PEG, scale bar = 200 nm

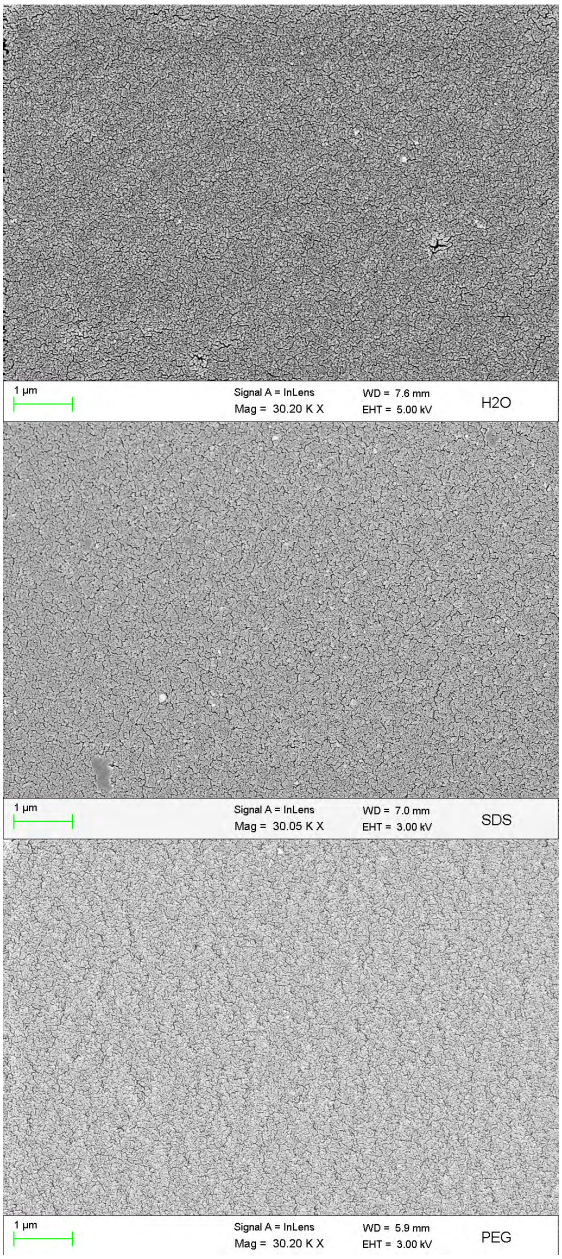

Figure 3.5: Films formed in H_2O at room temperature with additives. a. solution of cellulose/EMIMAc, scale bar = 3 μm; b. solution of cellulose/EMIMAc with SDS, scale bar = 2 μm; c. solution of cellulose/EMIMAc with PEG, scale bar = 2 μm

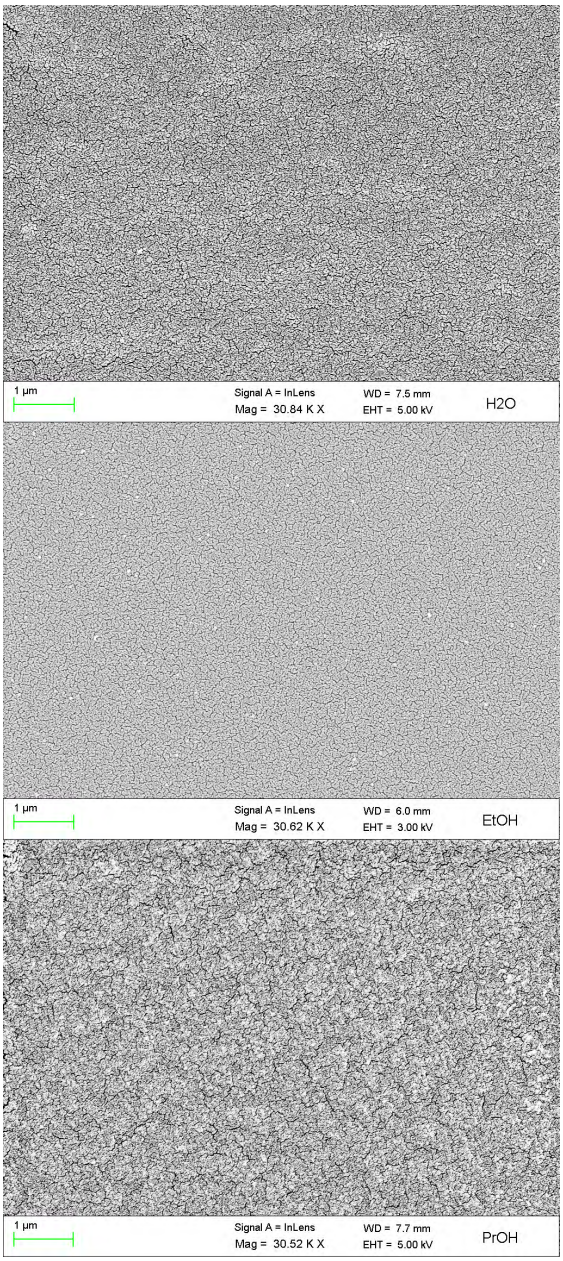

Figure 3.6: Films formed in different coagulants at room temperature. a. H_2O, scale bar = 1 μm; b. EtOH, scale bar = 1 μm; c. PrOH, scale bar = 1 μm

3.3 Fiber strength

Table 3.2 shows the tensile strength of the fibers both original and washed. These measurements were performed on a bundle of fibrils, whereas the standards refers to measurements on single fibrils It is shown that fibers spun in water at room temperature and PrOH gained larger density and stiffness. The tenacity values were far way from conventional fibers, for example Lyocell fibers have the tenacity above 40 cN/tex and cotton has the value of about 20 cN/tex(Söderlund, 2004). There were no significant differences between the PEG1 (not washed in a second bath) and PEG2 (washed in the second bath) fibers while the PEG2 fibers had a slightly increased elongation and stiffness.

Table 3.2: Table of the fiber tensile strength factors. F: load at break; ε: elongation at break; E^b indicates the fiber stiffness; Tex indicates the fiber linear mass density; Tenacity indicates the fibers strength; s: standard deviation. PEG1 refers to the fibers that were collected directly after the first bath which means were not washed in hot water while PEG2 did.

		F (N)		ε (%)		E^b (N/mm)	Tex (g/km)	Tenacity (cN/tex)
		a	s	a	s			
H_2O RT	Original	6.046	0.918	5.335	1.915	494.247	71.333	8.475
	Washed	6.471	0.920	4.753	2.294	455.525	71.848	9.007
EtOH	Original	3.878	0.590	5.436	2.453	320.747	46.000	8.431
	Washed	4.134	0.527	5.043	2.153	342.715	43.000	9.615
PrOH	Original	5.162	1.004	3.777	1.769	425.926	70.000	7.375
	Washed	5.417	0.701	5.270	2.463	406.727	63.000	8.598
H_2O hot	Original	2.189	1.162	2.421	1.321	214.852	46.256	4.732
	Washed	1.738	0,748	1.360	1.064	195.006	28.571	6.083
SDS	Original	2.462	0.544	2.696	2.496	252.468	27.970	8.803
	Washed	1.418	0.220	5.375	2.877	122.673	22.000	6.447
PEG1	Original	1.497	0.401	0.933	0.408	216.337	41.667	3.592
	Washed	1.885	0.571	1.300	0.826	226.820	35.639	5.289
PEG2	Original	2.348	0.478	2.179	0.928	241.161	41.000	5.728
	Washed	1.838	0.727	1.314	0.970	233.889	36.905	4.979

All fibers were dried after spinning (referred to as “original” in Figure 3.7), but to get rid of residual EMIMAc they were washed in water and dried (referred to as ”washed” in Figure 3.7).

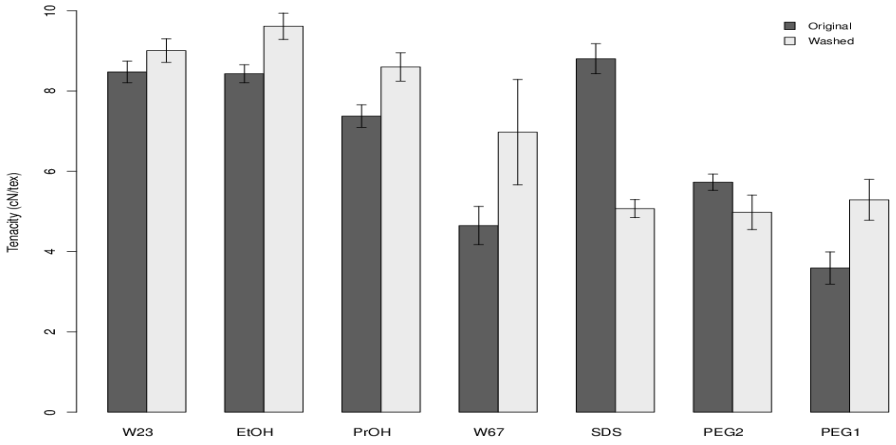

(a)

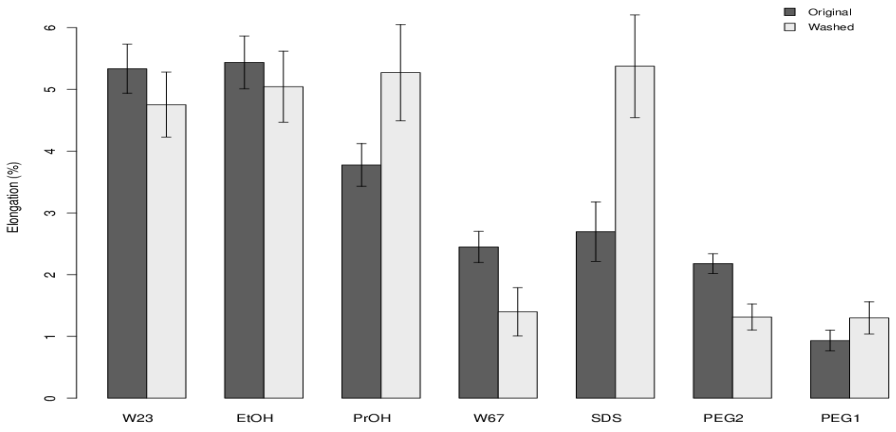

(b)

Figure 3.7: The tenacity (a) and elongation for original vs washed fibers

When taking a close look at the fibers strength after been washed, all fibers gained strength except the SDS and PEG2 fibers which lost strength (Figure 3.7a). PrOH and SDS fibers increased a lot their elongation; PEG1 fibers had a smaller increase while others decreased (Figure 3.7b). The reason for the big decrease in tenacity and increase in elongation for SDS is unclear, but a reasonable assumption may be that the SDS

molecule may be washed away and left some porous structures in the cellulose matrix or unordered cellulose chain structure which may weaken the fiber strength. Therefore how exactly SDS interacts with the cellulose molecules would be interesting for further studies. Some probe labeling techniques would be worth of trying in order to monitor the activities of SDS–cellulose, SDS–water and SDS–IL interactions.

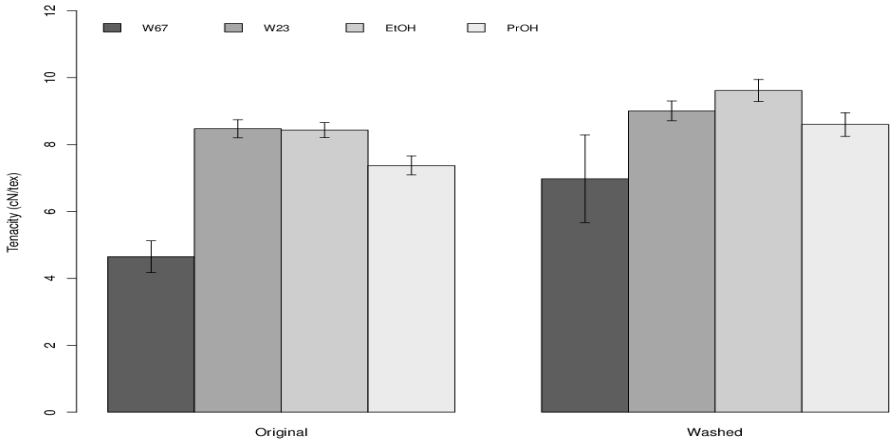

(a)

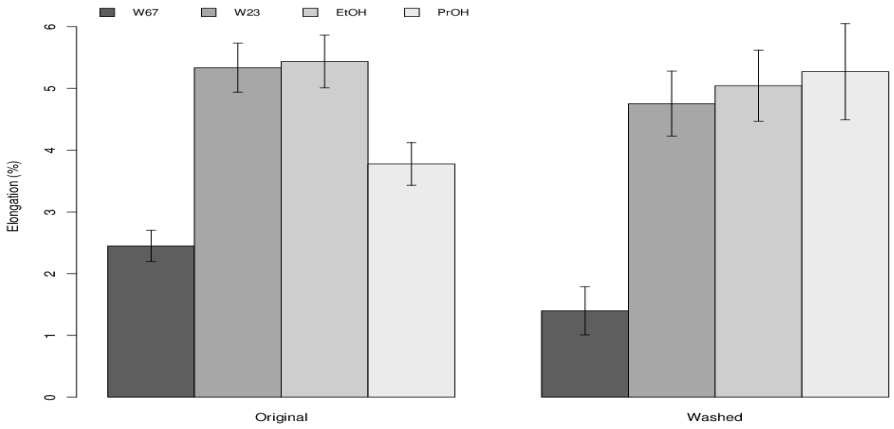

(b)

Figure 3.8: Cellulose coagulated in H_2O, EtOH and PrOH where in (a) the tenacity is plotted and in (b) the elogation is plotted.

It is clearly shown in Figure 3.8 that fibers spun in hot water revealed the weakest strength and elasticity compared to those fibers that were spun at room temperature. As is discussed previously, the miscibility is higher at a higher temperature, and the fiber

did not have much time to be stretched to obtain a more elongated structure, thus the fiber becomes weaker. Since only the fibers spun in water were comparable in the results, it would be interesting to spin the fibers with additives in water at room temperature too. PrOH fibers before wash were the weakest and had the least elasticity among the fibers at the same temperature condition however the result did not remain for those washed ones.

An explanation for this may be that PrOH makes the fiber coagulate slowly, leaving a more open structure of the cellulose. After washing, EMIMAc has been released and the cellulose chains may rearrange to form a more compact structure of the fiber.

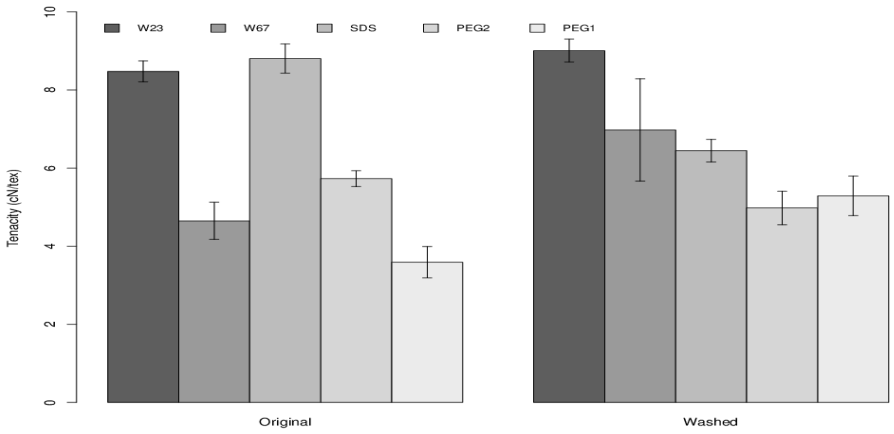

(a)

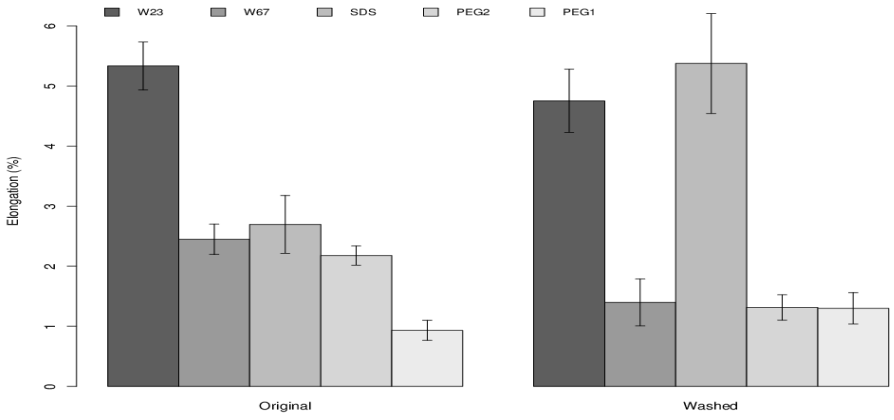

(b)

Figure 3.9: Cellulose with additives coagulated in hot water where in (a) the tenacity is plotted and in (b) the elogation is plotted.

Figure 3.9 compares the fibers with additives. The fibers spun in cold water were much stronger and better had higher elongation than most of other fibers. Surprisingly, the SDS fibers show much stronger strength before washing and the highest elasticity after washing compared to other fibers that were spun under the same temperature condition.

It should be reminded that the stretching speed after the first bath varied during the spinning process which may lead to some unclear results of the fiber strength from the different coagulants. Thus, a more controlled spinning processing including controlling the extruding pressure, coagulation bath temperature and the stretching speed are desired.

3.4 ESCA

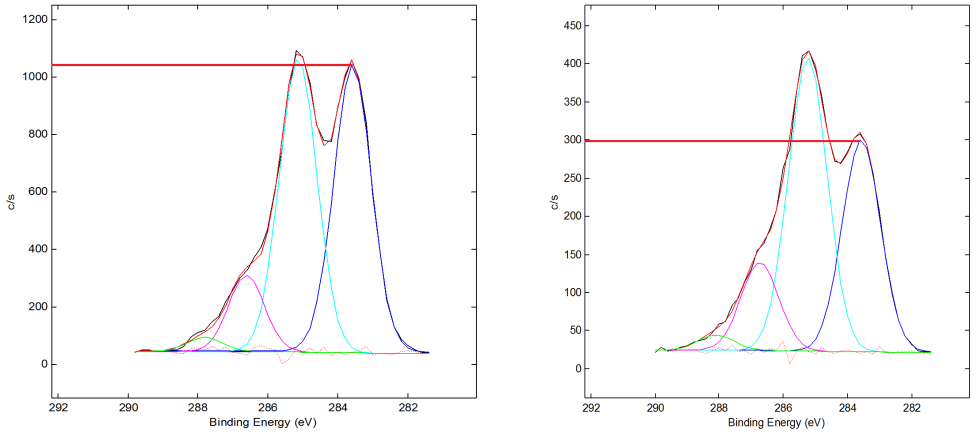

(a) Original **(b)** Washed

Figure 3.10: The chemical shift graph for fibers spun in water at room temperature. The indicated bindings from the right to the left according to Beamson and Briggs (1992) are: C–C binding, C–OH binding, O–C–O or C=O binding and O–C=O binding respectively. The count difference is about 700 before (a) and after washed (b).

From the ESCA analysis it was shown that the fibers seem to be contaminated by some unknown chemical compounds. Figure 3.10 shows the chemical shift in binding energy. The first blue peak to the right indicates some C–C bonding which means that the carbon only binds to other carbon, i.e. a quaternary carbon. However this kind of structure did not exist in any of the chemicals involved in this work. So the fibers were considered to be contaminated by something that has the C–C bonding structure (unknown compound) which may come from the fingers, gloves or somewhere else. The second light blue peak to the right indicates the C–OH which may be the hydroxyl groups from the cellulose. The third red peak to the right indicates the O–C–O binding or C=O binging which may also from the ether groups or oxidized group in the cellulose or the cation from EMIMAc. The green peak to the left indicates a O–C=O binding which may from the oxidized group in the cellulose or the cation from EMIMAc.

By subtracting the counts (y-axis in Figure 3.10) for the original fiber by the counts that were after washing, yielding the differences for the unknown compound had before and after washing, some results may be revealed. The list of differences is shown in Table 3.3. It shows a big difference for the fibers with additives which indicates that the unknown compound was difficult to be washed away for the fibers with additives, in an other word the unknown compound was hold by the fibers while washing, which exhibits the surface property. If the unknown compound is assumed to be hydrophobic then the surface should be also hydrophobic otherwise the surface would be hydrophilic if the unknown compound is hydrophilic. Most likely this so called contamination consists of both EMIMAc and finger grease.

Table 3.3: Count differences before and after washing in H_2O

Fibers	Original	Washed	Difference
H_2O RT	1000	300	700
EtOH	1400	800	600
PrOH	1400	900	500
H_2O hot	1100	650	450
SDS	700	600	100
PEG1	600	650	-50
PEG2	700	500	200

3.5 Contact angle

For several reasons contact angle measurements on cellulosic films/fibers were problamatic. It was very difficult to achieve an acceptable smooth film surface for the measurements, and moreover with water as the wetting agent, it was absorbed quickly by the film. This is why the measurements of CA of water on films was unsuccessful, however by using hexadecane as the wetting agent, some CA values were detected and is shown in Table 3.4. It should be noticed that only one angle was recorded successfully for the PEG film, but the values (Table 3.4) from the other films were average of 10 measurements. Since hexadecane is extremely hydrophobic, and the CAs were very low which indicates that the surface may be hydrophobic while SDS and PrOH films may reveal a less hydrophobic surface than the others since they had the highest CA in each group.

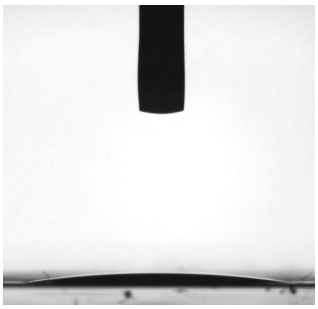

Figure 3.11: The image captured by the optical tensiometer: liquid: hexadecane, solid: film made with SDS

Due to the difficulties of handling the tensiometer for the measurements of th CA on fibers, the results were not representative and are not listed.

The hypothesis may be confirmed by comparing CA from films coagulated in H_2O and in EtOH. It also seems like SDS increased the hydrophilicity, whereas films from PrOH probably still were contaminated by EMIMAc and should be considered as an outlier.

Despite of the facts mentioned above, some other objective factors may also be taken into consideration, for example the purity of the MCC source, it was revealed that the Avicel MCC contains not only cellulose but also some other compounds like hemicellulose, lignin (personal contact), which may affect the fiber properties. The drying conditions should be kept constant and recorded, for example a certain hours or days under what kind of environment (the humility and temperature), if using the vacuum

drier the temperature and pressure should be kept constant as well.

Table 3.4: The table of CA on films

	H_2O	EtOH	PrOH	SDS	PEG
θ (°) (hexadecane)	13.241	5.332	7.934	12.633	9.894
	9.728	3.991	9.416	10.408	
	11.56	7.524	12.011	20.556	
	11.889	6.147	9.66	15.803	
	7.561	6.52	10.886	22.011	
	8.393	7.326	10.044	16.074	
	10.042	5.856	9.731	19.093	
	11.041	6.953	14.237	17.199	
	8.842	5.297	10.061	16.699	
	8.043	8.337	6.116	23.385	
	8.027	5.563	7.853	12.995	
a	9.634	5.749	11.185	14.663	9.894
s	1.871	1.233	2.166	4.048	

4

Conclusions and future work

The hydrophocity of the cellulose fiber surface might be directed by choosing a certain solvent in the precipitation bath and with some amphiphilic additives. Fiber tensile strength is also affected by the different approaches. Higher temperature gives a smoother surface but weaken the fiber strength. SDS gives smoother surface morphology, more hydrophilic surface and may also enhance fiber strength and elasticity.

To develop a desired fiber requires a lot of tails and testings, this diploma work was done in such a short time and many adjustments need to be made and more details need to be drawn in the right future. As discussed previously, the MCC impurities should be checked for better understanding of the revealed fiber properties, and a more controlled spinning process is needed to get comparable fibers. The results have drawn some attentions to the relationship between the surface smoothness and the fiber strength. The question of whether the surface smoothness reflects the structure of the inner core of the fiber and therefore the fiber strength may be answered by checking the cross section of the fibers. The contact angle measurements on fibers need to be carried out as soon as possible to get a more convinced result. In order to do so, a better sample handling which includes sample surface protection, and a well–defined cleaning process which will lead to more accurate and reliable results. Some probe labeling and ion detection technique would be interesting for understand the additive–cellulose, additive–IL and additive–non-solvent interactions, and some other additives like sodium dodecylbenzenesulfonate and sodium tetradecyl sulfate (STS) are worth trying to get a solid understanding of the hydrophobic interaction effects.

References

Attension. Contact Angle, 2011.

Roger Smart Stewart McIntyre Mike Bancroft. X-ray Photoelectron Spectroscopy, 2011.

G. Beamson and D. Briggs. *High resolution XPS of organic polymers: the Scienta ESCA300 database*. Wiley Chichester, UK, 1992.

Tao Cai, Huihui Zhang, Qinghua Guo, Huili Shao, and Xuechao Hu. Structure and properties of cellulose fibers from ionic liquids. *Journal of Applied Polymer Science*, 115(2):1047–1053, 2010.

Juan Chen, Chengguo Wang, Heyi Ge, Yujun Bai, and Yanxiang Wang. Effect of coagulation temperature on the properties of poly(acrylonitrile- itaconic acid) fibers in wet spinning. *Journal of Polymer Research*, pages 223–228, March 2007.

Susan K Cousins and R Malcolm Brown Jr. Cellulose I microfibril assembly: computational molecular mechanics energy analysis favours bonding by van der Waals forces as the initial step in crystallization. *Science*, 36(20):3885–3888, 1995.

E. Paul DeGarmo, J. T. Black, and Ronald A. Kohser. *Materials and Processes in Manufacturing*. Wiley, 2002.

H.Y. Erbil. *Surface chemistry of solid and liquid interfaces*. Wiley-Blackwell, 2006.

Fairbrother. X-ray photoelectron spectroscopy, 2004. URL `http://www.jhu.edu/~chem/fairbr/surfacelab/xps.html`.

Li Feng and Zhong-lan Chen. Research progress on dissolution and functional modification of cellulose in ionic liquids. *Journal of Molecular Liquids*, 142(1-3):1–5, August 2008.

A D French, D P Miller, and A Aabloo. Miniature crystal models of cellulose polymorphs and other carbohydrates. *International Journal of Biological Macromolecules*, 15(1): 30–36, 1993. URL `http://www.ncbi.nlm.nih.gov/pubmed/8443130`.

Dr. Karina Grundke, Dr. Victoria Dutschk, Stefan Michel, and Kathrin Pöschel. Contact angle Labs (sessile drops, captive bubbles, Axisymmetric Drop Shape Analysis-ADSA, Wilhelmy balance technique), 2011. URL `http://www.ipfdd.de/Contact-angle-Labs.1122.0.html?&L=0`.

B. S. Gupta. Surface Wetting Characteristics of Cellulosic Fibers. *Textile Research Journal*, 70(4):351–358, April 2000.

Frank Hermanutz, Frank Gähr, Eric Uerdingen, Frank Meister, and Birgit Kosan. New Developments in Dissolving and Processing of Cellulose in Ionic Liquids. *Macromolecular Symposia*, 262(1):23–27, January 2008.

Dieter Klemm, Brigitte Heublein, Hans-Peter Fink, and Andreas Bohn. Cellulose: fascinating biopolymer and sustainable raw material. *Angewandte Chemie (International ed. in English)*, 44(22):3358–93, May 2005.

Birgit Kosan, Christoph Michels, and Frank Meister. Dissolution and forming of cellulose with ionic liquids. *Cellulose*, 15(1):59–66, September 2007.

Ran Li, Chunyu Chang, Jinping Zhou, Lina Zhang, Wenqing Gu, Chuntao Li, Shilin Liu, and Shigenori Kuga. Primarily Industrialized Trial of Novel Fibers Spun from Cellulose Dope in NaOH/Urea Aqueous Solution. *Industrial & Engineering Chemistry Research*, 49(22):11380–11384, November 2010.

Björn Lindman, Gunnar Karlström, and Lars Stigsson. On the mechanism of dissolution of cellulose. *Journal of Molecular Liquids*, 156(1):76–81, September 2010.

C.S. Lovell, A. Walker, R.A. Damion, A. Radhi, S.F. Tanner, T. Budtova, and M.E. Ries. Influence of Cellulose on Ion Diffusivity in 1-Ethyl-3-Methyl-Imidazolium Acetate Cellulose Solutions. *Biomacromolecules*, 2010.

Antoinette C. O'Sullivan. Cellulose: the structure slowly unravels. *Cellulose*, pages 173–207, 1997.

Jim Schweitzer. Scanning electron microscope (sem), 2010. URL `http://www.purdue.edu/REM/rs/sem.htm`.

William Smith and Javad Hashemi. *Foundations of Materials Science and Engineering*. McGraw-Hill Science/Engineering/Math, 2005.

Susan Swapp. Scanning electron microscopy (sem), 2010. URL `http://serc.carleton.edu/research_education/geochemsheets/techniques/SEM.html`.

Carl-Axel Söderlund. Man-made textile fibres, 2004.

CAI Tao, Z. Hui-hui, GUO Qing-hua, S. Hui-li, and HU Xue-chao. Effect of Spinning Process on the Performance of New Cellulose Fiber from Ionic Liquids. *Synthetic Fiber in China*, 38(5):11–14, 2009.

Cate Wallace and Scott J. Robinson. How ESEM Works, 2011.

F Wendler, Z Persin, and K Stana-Kleinschek. Morphology of polysaccharide blend fibers shaped from NaOH, N-methylmorpholine-N-oxide and 1-ethyl-3-methylimidazolium acetate. *Cellulose*, 2011.

Chihiro Yamane, Takeshi Aoyagi, Mariko Ago, Kazuishi Sato, Kunihiko Okajima, and Toshisada Takahashi. Two Different Surface Properties of Regenerated Cellulose due to Structural Anisotropy. *Polymer Journal*, 38(8):819–826, 2006.

Shuai Zhang, Fa-Xue Li, and Jian-Yong Yu. Structure and Properties of Novel Cellulose Fibres Produced From NaOH/PEG-treated Cotton Linters. *Iranian Polymer Journal*, 19(12):949–957, 2010.

A

Appendix

A.1 Manual for making the films

In this session, a series of steps for making cellulose films are described. To demonstrate the procedures, the cellulose solution without additives is used and the coagulation bath is water.

A.1.1 Preparation

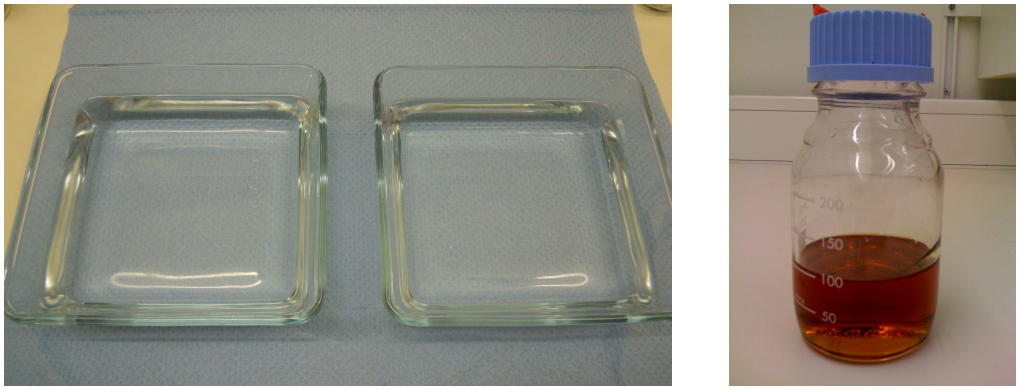

(a) Coagulation bath **(b)** Cellulose solution

Figure A.1: Prepare the coagulation bath in two bowls with about 300 ml in volume and the cellulose solution.

A.1.2 Actual step for making the films

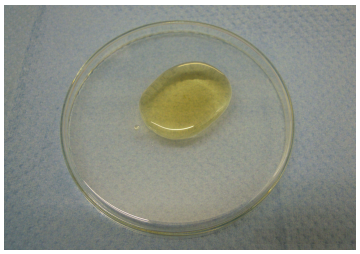

(a) Two gram cellulose solution on a petri dish

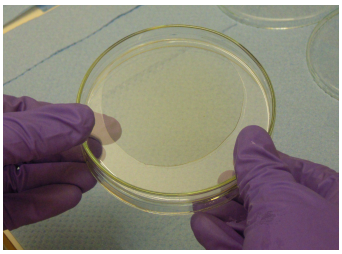

(b) Making the film

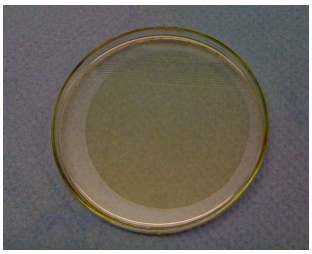

(c) Film size

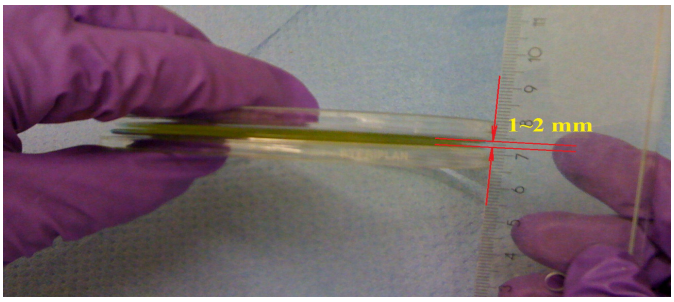

(d) Thickness: about 1–2 mm

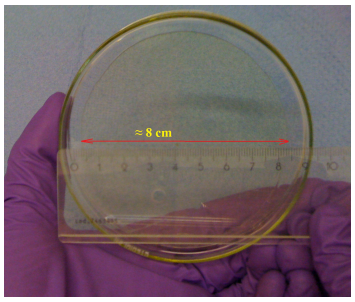

(e) Film size about 8 cm

Figure A.2: Weight approximately 2 g of the solution on the back side of a petri dish. Make sure there are as few bubbles as possible and put another one on top of the solution and press them until the diameter reaches approximately 8 cm in order to make a thin film, and the thickness reaches about 1–2 mm.

A.1.3 Coagulation

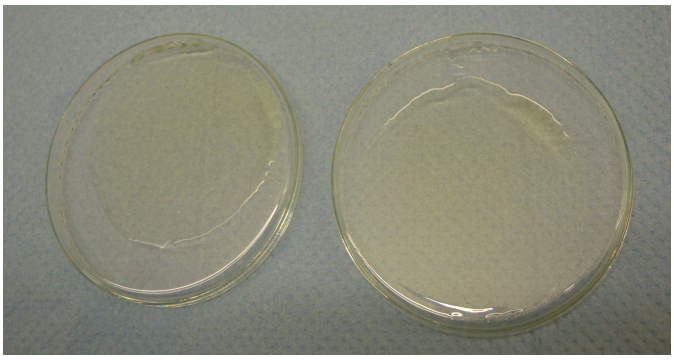

(a) Before coagulation

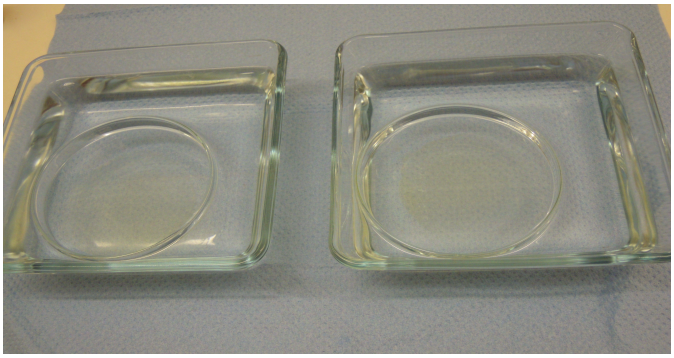

(b) Coagulation with water

(c) Coagulation with volatile solvents

Figure A.3: (a) Slide the one of the petri dishes way carefully and wait for about 30 s in order to let the solution settle on the petri dishes and get a smooth surface; (a) put the petri dished in the coagulation bath prepared in Step A.1.1; (c) ammonia foil is need for EtOH and PrOH or other volatile solvents as the coagulation bath. The coagulation time varies on different coagulation bath. At least 10 min is recommended in order to get a fully precipetated film.

A.1.4 Drying

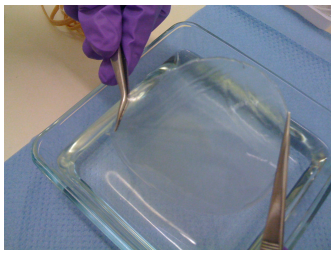

(a) The film has been formed

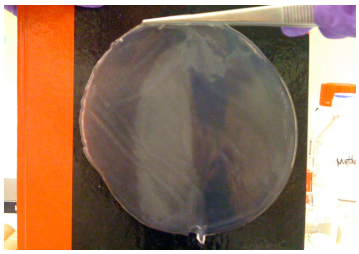

(b) Mostly transparent

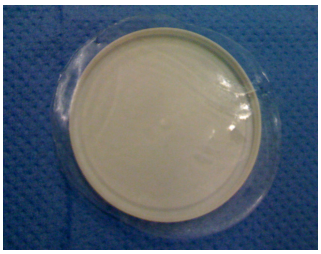

(c) Film on a lid

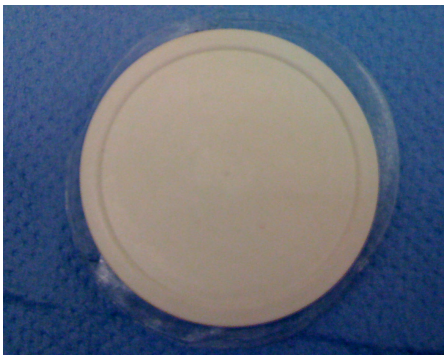

(d) Cover with another lid

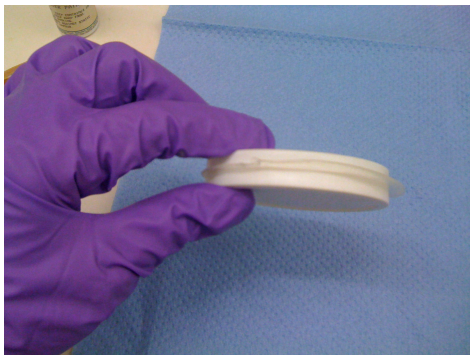

(e) The film is between the two lids

Figure A.4: (a) Carefully take out the film by the help of tweezers; (b) the film looks mostly transparent; (c) put the film over a lid or a petri dish which should has smaller diameter so it can hold the film; (d) cover the film with another lid or petri dish; (e) so the film is suspended between them in order to avoid the shrinking while drying. It is needed at least one day for air–drying or vacuum dry over night.

A.1.5 The film

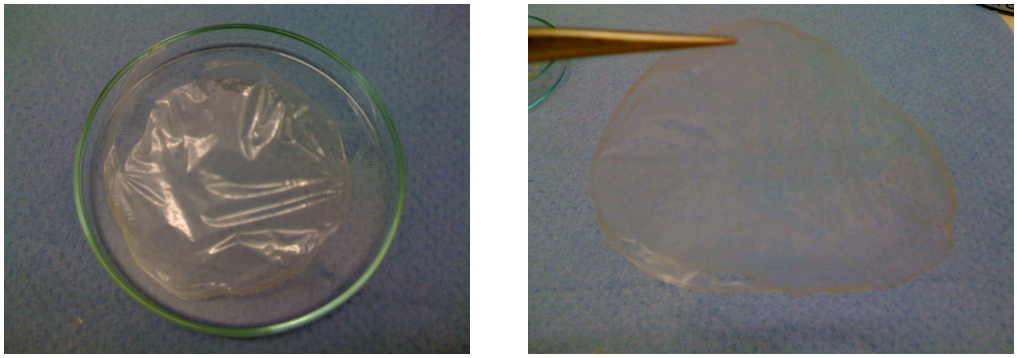

(a) **(b)**

Figure A.5: After the film is dried, carefully removed the lids and transport it to a clean place, e.g. in a petri dish with cover, for furthur characterization.